JOURNAL OF SOLID STATE CHEMISTRY 116, 1–7 (1995)

A Single-Crystal Study of the Magnetic Behavior and Exchange Coupling in $Cu_2(OH)_3NO_3$

G.-G. Linder,* M. Atanasov,†,[1] and J. Pebler*

*Fachbereich Chemie und Zentrum für Materialwissenschaften der Philipps-Universität, Hans-Meerweinstr., D-35032 Marburg, Germany; and †Institute of General and Inorganic Chemistry, Bulgarian Academy of Sciences, BI.11, Sofia 1113, Bulgaria

Received November 18, 1993; in revised form April 29, 1994; accepted May 7, 1994

Single-crystal magnetic susceptibilities of the title compound as a function of the magnitude and orientation of the magnetic field are reported. The temperature behavior of χ above the phase transition is described in terms of the Bonner–Fischer model for linear chains. On the basis of the experimental results and calculations within the Hückel model, it may be concluded that linear magnetism arises from pronounced antiferromagnetic exchange coupling of Cu(2) sites within chains parallel to the crystallographic *b*-axis. © 1995 Academic Press, Inc.

I. INTRODUCTION

The optical and structural properties of layered transition metal hydroxide nitrates have been extensively studied (1–4). However, little attention has been paid to their magnetic behavior. In this respect, the monoclinic compound $Cu(OH)_3NO_3$ is an interesting model system. Its structure (5) is similar to that of $Mg(OH)_2$, where one-fourth of the OH^- groups are substituted by nitrate ligands in an ordered way. Copper(II) occupies two nonequivalent positions. Site one [Cu(1)] is coordinated by four equatorial OH^- groups and two NO_3^- groups in *trans* positions. In site two, [Cu(2)] is coordinated by five OH^- groups and one NO_3^- group. The Cu(1) and Cu(2) sites form chains parallel to the crystallographic *b*-direction. The bridging geometry of the $Cu(1)O_6$ octahedra consists of one OH^- group and one oxygen from the NO_3^- group (Fig. 1), while the $Cu(2)O_6$ octahedra are connected by two OH^- groups to each other. Neighboring Cu(1) and Cu(2) are bridged in two different ways (via two hydroxo groups or via one hydroxo group and an oxygen atom of the NO_3-group), alternating along the direction of the b-axis.

Magnetic interactions in dihydroxo-bridged Cu^{2+} dimers have been extensively studied, both experimentally (6) and theoretically (7). The magnetic coupling changes from ferromagnetic to strong antiferromagnic with increasing Cu–OH–Cu bridging angle. On the basis of the structural data (bridging angles α varying between 100° and 110°), it is therefore expected that antiferromagnetic coupling between Cu centers will take place, and this was supported by recent ESR measurements (8) on Cu(II)–Mg(II) hydroxide nitrate solid solutions. However, the CuO_6 polyhedra are rather distorted, and no quantitative arguments about the magnetic exchange between the various Cu ions could be made. The exchange coupling between magnetic ions in a regular triangular arrangement is known to be the subject of a strong frustration interfering with the magnetic ordering (9a). In particular, systems such as Cu(II) with $S = \frac{1}{2}$ have been found to be subject to large quantum fluctuations without long-range order in the ground state (9b). It was therefore interesting to see how the presence of alternating Cu(1) and Cu(2) chains within a sheet in $Cu(OH)_3NO_3$ and with possibly different exchange constants could modify the magnetic behavior of such systems.

Here we report on single-crystal magnetic susceptibility measurements as a function of the temperature, and the dependence of χ_m on the magnitude and direction of the magnetic field. This information will be used together with a theoretical analysis in order to gain information about the exchange coupling between Cu^{2+} centers in $Cu(OH)_3NO_3$. We intend to show that the magnetic behaviour is governed by antiferromagnetic coupling in the chains of bi-hydroxo-bridged Cu(2) ions and weaker exchange coupling within the Cu(1) chains and exchange between Cu(1) and Cu(2). Thus we deal with a unique example of a linear magnetic system within a layered structure of magnetic ions.

II. EXPERIMENTAL

II.1. Sample Preparation

Water solutions of 2 *M* $Cu(NO_3)_2$ and 1 *M* $Mg(NO_3)_2$ were mixed in a volume ratio of 1 : 1 and filled in a platinum

[1] To whom correspondence should be addressed at: Institute für Theoretische Chemie, Heinrich-Heine Universität, Universitätsstrasse 1, Geb.26.32, D-40225 Düsseldorf, Germany.

0022-4596/95 $6.00

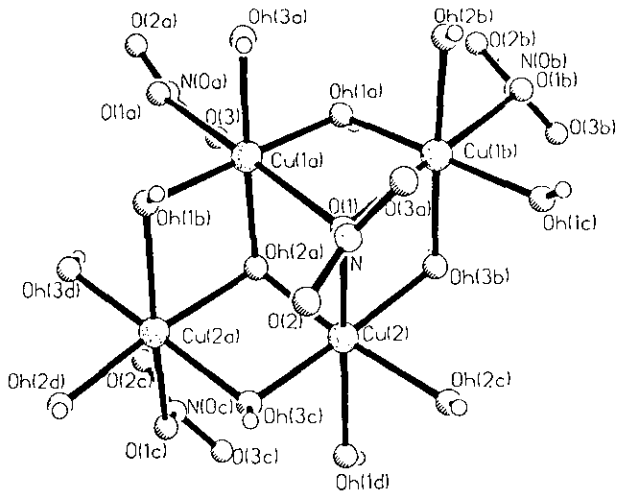

FIG. 1. Structural sketch of the $Cu_2(OH)_3NO_3$ layers along the c-axis.

autoclave; 0.6 g of Cu chips was added to 14 ml of the above mixed solution. All substances used were of "pro analysi" quality. The autoclave was sealed and held at 300°C for 14 days at an autogenious pressure of ≈84 bar. Large (up to 5 × 3 × 0.4 mm) transparent green thin plates were obtained. The crystals were washed with water and dried at 80°C.

II.2. Chemical Analysis

Qualitative chemical analysis with a scanning electron microscope showed no traces of Mg in the crystals.

II.3. X-Ray Diffraction Analysis and Sample Mounting

X-ray powder analysis revealed a diffraction pattern identical with the monoclinic structure of $Cu_2(OH)_3NO_3$ found by Effenberger (5).

A crystal of a size 2 × 1 × 0.3 mm was oriented by using a Bürger precession technique with respect to the crystallographic axes a, b, and c^* (Fig. 2). Since the monoclinic angle $\beta = 94°29'$ differs only slightly from 90°, in the subsequent discussion we assume that within the error limits (adjustment of the crystal in the magnetic field within 2°) c^* is identical to c. For single-crystal magnetic measurements, the crystal was embedded in the synthetic resin Araldite [Bisphenol-A-(Epichlorhydrin) Epoxy Resin MW ≤ 700, available from Ciba Geigy]. For the high-temperature measurements up to 400 K, a powdered sample in a quartz holder was used.

II.4. Magnetic Susceptibility Measurements

Single-crystal magnetic susceptibilities at field strengths of 50 G, 10 kG, and 30 kG and a field direction parallel to the a, b, and $c(c^*)$ axes were measured between 1.8 and 400 K using a SQUID magnetometer (Quantum Design). At 5 K, field dependence measurements in all three crystallographic directions have been made from zero field up to 50 kG. Diamagnetic corrections were made for the Araldite sample holder (empirically) and the sample itself (10).

II.5. Model Calculations

Exchange coupling energies between Cu^{2+} centers were calculated within the extended Hückel (EH) model (11) using the approach of Hay *et al.* (12). Within this method, the coupling between two equivalent magnetic orbitals φ_1 and φ_2, b_{12} is approximated by their energy splitting ΔE in forming the corresponding molecular orbitals:

$$b_{12} = \Delta E/2. \qquad [1]$$

Exchange coupling of orbitals located at magnetically inequivalent sites (e.g., Cu(1)–C(2)) can be deduced from the expression

$$b'_{12} = [(E_1 - x)(E_2 - x)]^{1/2}, \qquad [2]$$

where x is the MO energy of the Cu(1)–Cu(2) dimer, while E_1 and E_2 are the baricenter energies of Cu(1) and Cu(2) in the Cu(1)–Cu(1) and Cu(2)–Cu(2) dimers, respectively. The singlet–triplet energy separation $2J_{12}$ is calculated from b_{12} and the Coulomb repulsion energy U as follows:

$$J_{12} = -2b_{12}^2/U. \qquad [3]$$

Extended Hückel calculations were performed using a computer program by Calzaferri *et al.* (13). A full account of the exact geometry of nearest neighbor surroundings

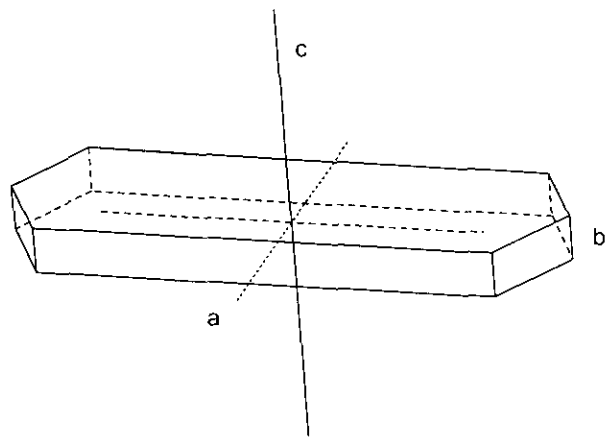

FIG. 2. Single-crystal orientation with respect to the crystallographic axes.

TABLE 1
Atomic Parameters for MO Calculations

Atom	Orbital	H_{ii} (eV)	ζ_1	ζ_2	c_1^*	c_2^*
Cu	3*d*	−14.00	5.95	2.30	0.593	0.574
	4*s*	−11.4	2.2	—	1.0	—
	4*p*	−6.06	2.2	—	1.0	—
O	2*p*	−14.8	2.275	—	—	—
N	2*p*	−13.4	1.95	—	—	—
H	1*s*	−15.0	2.20	—	—	—

of Cu(1) and Cu(2) (Fig. 1) was made on the basis of atomic coordinates from structural data (5). Atomic orbital energies and wavefunction exponents are specified in Table 1.

III. RESULTS AND DISCUSSION

III.1. Magnetic Susceptibilities

The magnetic susceptibility of a powdered sample as a function of the temperature at a field strength of 10 G is given in Fig. 3. The data show a maximum at about 7 K. The high-temperature part follows Curie–Weiss behavior, as seen by the $1/\chi$ versus T plot in the same figure. An effective moment of 1.75 μ_B of Cu(2+) is found. This value corresponds to an essentially unchanged spin-only value ($S = \frac{1}{2}$, $\mu = 1.73\mu_B$). The Curie–Weiss constant ($\Theta_p = -8(1)$ K) is in agreement with an antiferromagnetic coupling interaction.

No effective difference of the magnetic susceptibility was noticed at 30 kG. The single-crystal magnetic susceptibility χ as a function of temperature at $H = 10$ and 30 kG with a magnetic field parallel to the *a*, *b*, and *c* and crystallographic axes is shown in Figs 4a, 4b, respectively. There is a clear difference in the behavior of the magnetic susceptibility in the low-temperature region (below the maximum) for the two settings of the magnetic field. It seems that at $H = 30$ kG, the internal magnetic coupling which is particularly pronounced in the $H \parallel b$ curve at $H = 10$ kG, is overpowered by the applied field. The slight susceptibility increase with decreasing temperature is indicative of a prevalent antiferromagnetic coupling along the *b*-direction, i.e., parallel to the Cu(1)–Cu(1) and Cu(2)–Cu(2) chains with possible spin orientations perpendicular to *b*. A small difference is also seen for $H \parallel a$ and $H \parallel c$ directions. It is noteworthy that there is a reasonably reproducible reversibility of the temperature behavior of the susceptibility, as illustrated in Fig. 5 for a magnetic field of 50 G with H along the *c*-direction. Similar reversibility is also obtained for $H \parallel a$ and $H \parallel b$, thus indicating no or a negligible ferromagnetic component.

Field dependence measurements gave no indication of a frustrated system.

III.2. Magnetic Exchange Coupling in $Cu_2(OH)_3NO_3$

We restricted the consideration to dimeric pairs, taking full account of the coordination geometry (Fig. 1). A list of coupling energies and antiferromagnetic exchange con-

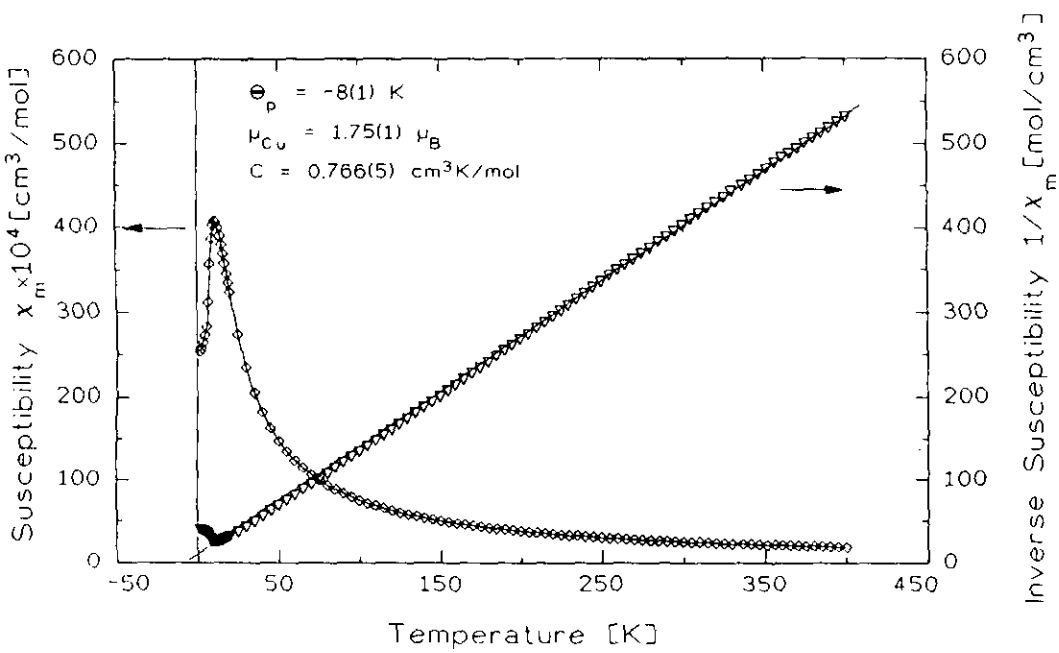

FIG. 3. Powder magnetic susceptibility dependence on temperature (1.8–400 K); $H = 10$ kG.

TABLE 2
Coupling Energies and Antiferromagnetic Exchange Constants for Cu^{2+} Dimers in $Cu_2(OH)_3NO_3$

Cluster	Bridging atoms	x_- (eV)	x_+ (eV)	E (eV)	ΔE	J_{12} (cm^{-1})[a]
Cu(1)–Cu(1)	OH^-, ONO_2^-	−12.957	−12.783	−12.870	0.174	−24
Cu(2)–Cu(2)	2 OH^-	−13.174	−12.799	−12.986	0.375	−111
Cu(1)–Cu(2)	2 OH^-	−13.024	−12.815	−12.919	0.180	−26
Cu(2)–Cu(1)	OH^-, ONO_2^-	−13.061	−12.799	−12.930	0.234	−43

[a] Calculated with a U-value for Cu^{2+} of 5.1 eV; see J. Zaanen and G. A. Sawatzky, *J. Solid State Chem.* **88**, 8–27 (1990).

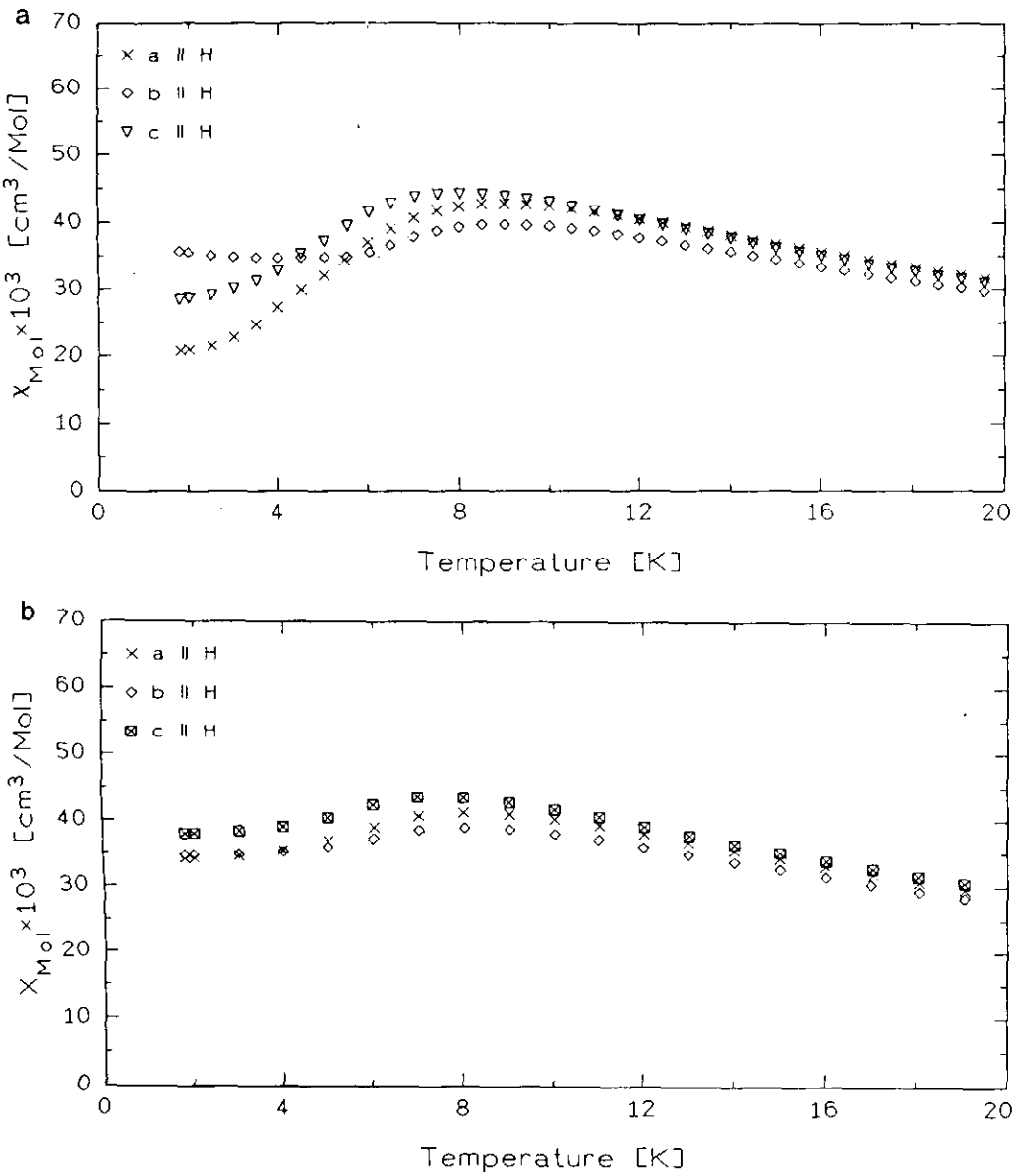

FIG. 4. Single-crystal low-temperature magnetic susceptibility dependence on temperature (1.8–30 K). The slight differences of the susceptibilities at higher temperatures are due to adjustment variations. (a) H = 10 kG; (b) H = 30 kG.

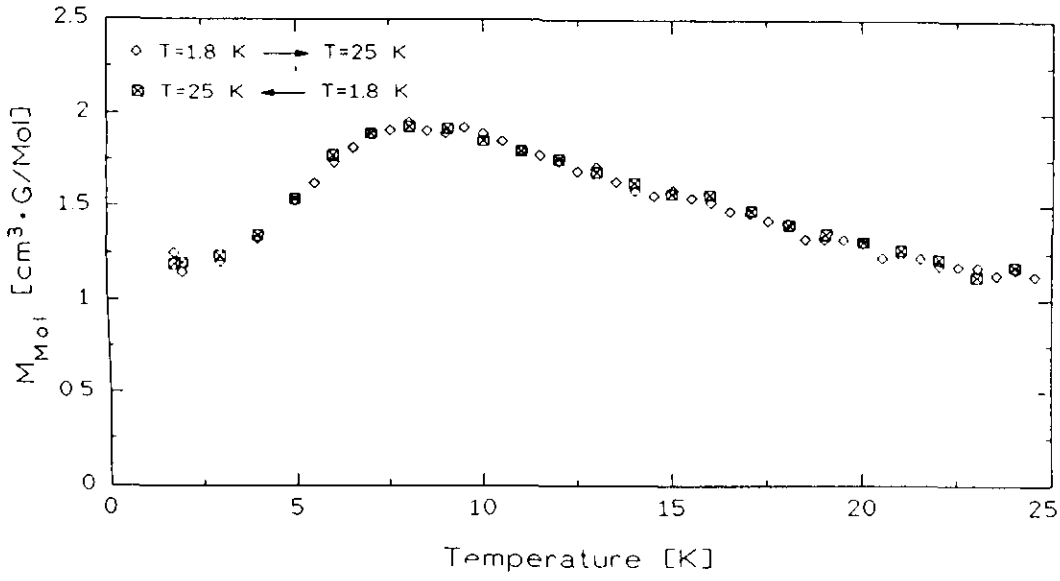

FIG. 5. Reversibility of low-field ($H \parallel c$, 50 G) magnetization vs temperature.

stants for Cu dimers is given in Table 2. Our results clearly show that for an environment which takes full account for the H and NO_2 moiety attached to the ligating oxygen atoms, the coupling of the bi-hydroxo-bridged Cu(2) ions is dominant followed by a less effective coupling between the Cu(1)–Cu(1) and Cu(1)–Cu(2) magnetic centers. The same qualitative result is obtained if only nearest neighbors coordinated to Cu^{2+} (i.e., CuO_6 polyhedra) are taken into account.

III.3. Discussion

The superexchange coupling of Cu^{2+} ions within the chains manifested by the χ vs T dependence on the one hand, and the low temperature of the susceptibility maximum (T = 7 K) on the other hand, suggest that $Cu_2(OH)_3NO_3$ has the behavior of a low-dimensional system (14, 15).

We studied the effect of spin coupling between the various pairs of Cu^{2+} ions [Cu(2)–Cu(2), Cu(1)—Cu(2), Cu(1)–Cu(1)] on the magnetic behavior, calculating explicitely spin multiplet energies and magnetic susceptibilities vs temperature for a cluster of Cu^{2+}, $s = \frac{1}{2}$ spins with the following topology:

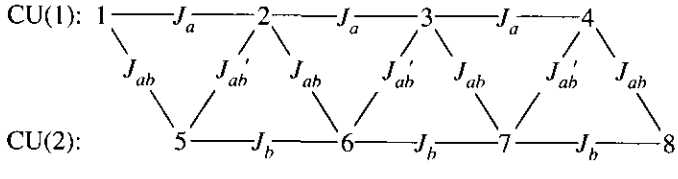

In order to account for the periodicity condition, interaction terms between pairs of magnetic ions (1, 4) (5, 8), and (1, 8) (via J_a, J_b, and J'_{ab}, respectively) have been introduced. Applying the exchange operator to the manifold of the 256 spin functions, it was possible to study explicitely the effect of the sign and magnitude of the model parameters J_a[Cu(1)–Cu(1)], J_b[Cu(2)–Cu(2)], J_{ab} [Cu(1)–Cu(2), bringing via two OH-groups], and J'_{ab}[Cu(1)–Cu(2), bridging via one OH^- and one NO_3-group] on the temperature dependence of the magnetic susceptibility.

A maximum in the susceptibility curve at low temperatures, as found by the experiment, could be only achieved by an antiferromagnetic interaction within one of the chains, accompanied by a far weaker antiferromagnetic coupling in the other chain. This is supported by the calculated exchange coupling constants within the EH model, suggesting that it is the Cu(2)–Cu(2) (J_b) coupling which has to be attributed to the stronger antiferromagnetic coupling, while both Cu(1)–Cu(1) (J_a) and Cu(1)–Cu(2) (J_{ab}, J'_{ab}) are to be ascribed as the weaker interactions. Our susceptibility plot shows (Fig. 6) that increasing the exchange coupling between Cu(1)–Cu(1) and Cu(1)–Cu(2) pairs [fixing the larger antiferromagnetic Cu(2)–Cu(2) coupling at $J_b = -10\ cm^{-1}$] leads to a shift of the maximum of the susceptibility to higher temperatures, accompanied by a lowering of χ_{max}. This is a convincing argument in favor of an one-dimensional model compared to a two-dimensional one (with comparable values of the coupling energies between the different Cu^{2+} ions). On the basis of our results, we can also exclude ferromagnetic coupling for Cu(1)–Cu(1) and Cu(2)–Cu(2) pairs, in which case the maximum in the susceptibility curve completely disap-

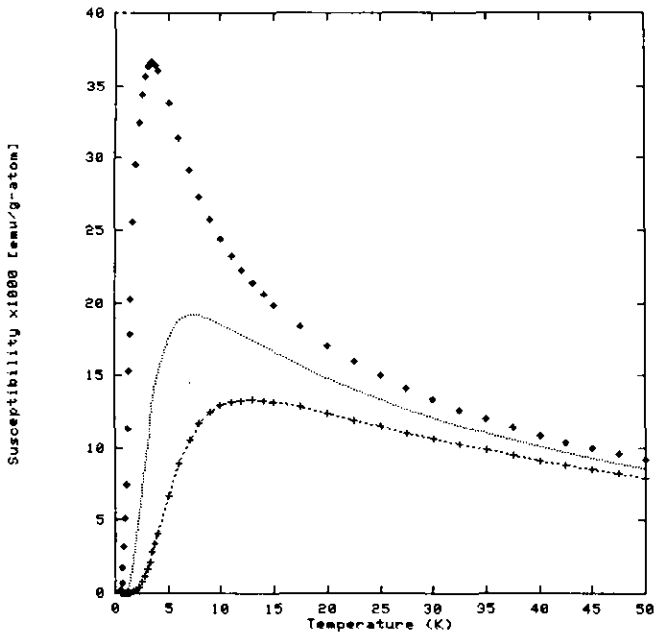

FIG. 6. Calculated temperature dependence of the susceptibility for a cluster of Cu^{2+} ions (described in the text) and different strengths of the antiferromagnetic coupling J between Cu(1)–Cu(1) and Cu(1–Cu(2) pairs of neighboring ions: $J = -1.5$ cm^{-1}, (points); $J = -3$ cm^{-1} (dots); $J = -5$ cm^{-1} (lines–plus). J_b [Cu(2)–Cu(2)] was fixed at -10 cm^{-1} in all curves.

peared. In support of this interpretation, we were able to reproduce faily well the χ vs T dependence using a one-dimensional model.

Assuming isotropic exchange, the Hamiltonian for a chain is

$$H = -2J \sum_i S_i S_{i+1}, \qquad [4]$$

with $S_i = S_{i+1} = \frac{1}{2}$. Hall (16) [see also (17)] has shown that the magnetic susceptibility as a function of temperature given by Bonner and Fisher (18) could be fitted by the expression

$$\chi = (Ng^2\mu_B^2/kT)\frac{[A + Bx + Cx^2]}{[1 + Dx + Ex^2 + Fx^3]}, \qquad [5]$$

where $A = 0.25$, $B = 0.14995$, $C = 3.0094$, $D = 1.9862$, $E = 0.68854$, $F = 6.0626$, and $x = |J|/kT$.

The plot in Fig. 7 displays a rather nice fit of the experimental data for an exchange coupling constant $J/k = -5.5(2)$ K, $g = 2.05$, and a maximum of χ at $T = 7.4(3)$ K. It should be noted that, a simulation of the χ vs T curve using a two-dimensional model for a Heisenberg system (19, 20) was also possible. However, this cannot be reconciled with our analysis of the underlying exchange coupling energies. The clear anisotropy of the susceptibility beginning even before the maximum (Fig. 4) is caused by the anisotropy of the crystal field, as evidenced by a study of the ligand field and ESR spectra of $Mg_xCu_{(2-x)}(OH)_3NO_3$ solid solutions (8). Using the reported g-values for isolated Cu(1) centers [$g_z = 2.315$, $g_{x,y} = 2.055$ (8)] and similar but slightly enlarged values for Cu(2), g-values along the crystallographic a, b, and c axes have been calculated for Cu(1) and Cu(2) using the following approximate expressions:

$$\text{Cu(1):} \quad g_a^2 = \tfrac{1}{6}(g_z^2 + 5g_{x,y}^2)$$
$$g_b^2 = \tfrac{1}{2}(g_z^2 + g_{x,y}^2)$$
$$g_c^2 = \tfrac{1}{3}(g_z^2 + 2g_{x,y}^2)$$
$$\text{Cu(2):} \quad g_a^2 = \tfrac{1}{3}(2g_z^2 + g_{x,y}^2)$$
$$g_b^2 = g_{x,y}^2$$
$$g_c^2 = \tfrac{1}{3}(g_z^2 + 2g_{x,y}^2).$$

It follows from these equations that the direction along the b-axis is the only one in which for Cu(2) the larger g_z do not contribute, yielding the smallest value of $g_b = g_{x,y}$. The same result is valid if an effective g-value taken as the average from the g-values of sites Cu(1) and Cu(2) is calculated. This is in excellent agreement with our data, yielding the lowest χ-values at higher temperatures for the magnetic fields parallel to b.

Below 5 K the anisotropy increases strongly, which may be indicative for the onset of 3D ordering. However, this has to be explicitely proved in further studies.

IV. CONCLUSIONS

On the basis of the present results, we were able to characterize $Cu_2(OH)_3NO_3$ as a low-dimensional magnetic

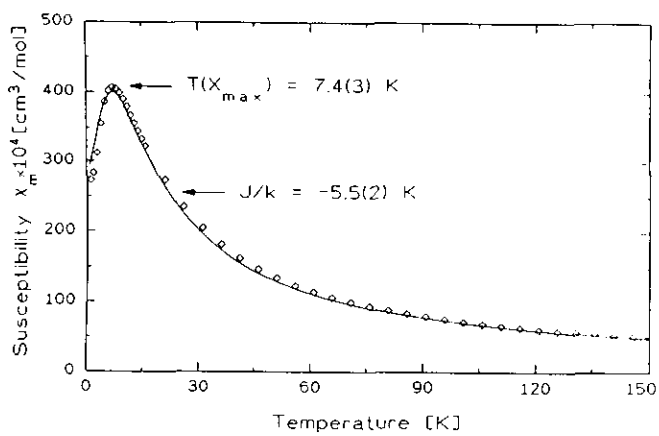

FIG. 7. Bonner–Fischer simulations of the χ vs T dependence.

system. An interpretation of these results using model calculations relates this behavior to antiferromagnetic exchange coupling which dominates in the Cu(2)–Cu(2) chains within the layered structure. However, further experiments including optical birefrigency on single crystals are highly desirable for a full characterization of the anisotropic behavior. In particular, such experiments as well as measurements on the magnetic contributions to the heat capacity will help to decide whether a magnetic ordering takes place and, if so, what kind. Such experiments are in progress.

ACKNOWLEDGMENTS

We owe thanks to the Alexander von Humboldt Foundation (M. Atanasov) and Fonds der Chemischen Industrie (G.-G. Lindner) for financial support. Thanks are due to Prof. Dr. D. Reinen (University of Marburg) for illuminating discussions and encouragement. We thank C. Frommen for valuable help with the magnetic measurements.

REFERENCES

1. K. Petrov and L. Markov, *Silikattechnik* **37,** 197 (1986).
2. N. Zotov and K. Petrov, *Z. Kristallogr.* **190,** 235 (1990).
3. N. Zotov, K. Petrov, Dimitrova-Pankova, *J. Phys. Chem. Solids* **51,** 1199 (1990).
4. N. Zotov, K. Petrov, and S. Hristov, *Thermochim. Acta.* **198,** 61 (1992).
5. H. Effenberger, *Z. Kristallogr.* **165,** 127 (1983).
6. D. J. Hodgson, *Prof. Inorg. Chem.* **19,** 173 (1975).
7. M. Atanasov, S. Angelov, and I. Mayer, *J. Mol. Struct. (Theochem.)* **187,** 23 (1989).
8. M. Atanasov, N. Zotov, C. Friebel, K. Petrov, and D. Reinen, *J. Solid State Chem.* **108,** 37 (1994).
9. (a) R. S. Gekht, *Sov. Phys. JETP* **75,** 1058 (1992); (b) P. W. Anderson, *Science* **235,** 1196 (1987).
10. E. König and G. König, "Magnetic Properties of Coordination and Organometallic Coordination Compounds." Landolt–Börnstein, New Series, Vol. II-8, Springer, Berlin/Heidelberg/New York, 1976.
11. R. Hoffman, *J. Chem. Phys.* **39,** 1397 (1963).
12. P. J. Hay, J. C. Thibeault, and R. Hoffmann, *J. Am. Chem. Soc.* **97,** 4884 (1975).
13. (a) G. Calzaferri, L. Forss, and I. Kamber, *J. Phys. Chem.* **93,** 5366 (1989); (b) G. Calzaferri and M. Brändle, *QCPE Bull.* **12,** No. 4 (1992).
14. R. L. Carlin, "Magnetochemistry," Chap. 7. Springer-Verlag, Berlin, 1986.
15. R. D. Willett, D. Gatteschi, and O. Kahn (Eds.), "Magneto-Structural-Correlations in Exchange Coupled Systems." NATO ASI Series, Reidel, Dordrecht 1985.
16. J. W. Hall, Ph.D. Dissertation, University of North Carolina, 1977.
17. W. E. Hatfield and E. R. Jones, *Inorg. Chem.* **9,** 1502 (1970).
18. J. C. Bonner and M. E. Fisher, *Phys. Rev. A* **135,** 640 (1964).
19. G. S. Rushbrooke and P. J. Wood, *Mol. Phys.* **1,** 409 (1963).
20. M. E. Lines, *J. Phys. Chem. Solids* **31,** 101 (1970).